Manuscript M7:01316-REVISED
Journal of Biological Chemistry
July 29, 2007

Attenuated Free Cholesterol Loading-Induced Apoptosis but Preserved Phospholipid Composition of Peritoneal Macrophages from Mice that Do Not Express Group VIA Phospholipase A_2

Shunzhong Bao[a], Yankun Li[b], Xiaoyong Lei[a], Wu Jin[a], Mary Wohltmann[a], Alan Bohrer[a], Clay F. Semenkovich[a], Sasanka Ramanadham[a], Ira Tabas[b], and John Turk[a+]

SUPPLEMENTAL MATERIALS

Characterization of the complex lipid composition of peritoneal macrophages from wild-type and iPLA$_2$β-null mice by ESI/MS/MS. One potential explanation of the differential sensitivity of wild-type and iPLA$_2$β-null macrophages to free cholesterol loading-induced apoptosis is that they might differ in complex lipid composition. Some have proposed that iPLA$_2$β is a housekeeping enzyme involved in arachidonic acid incorporation into GPC lipids, phospholipid remodeling, and GPC lipid homeostasis (24-27). Data in Figures 9-12 in the body of this manuscript indicate that the GPC lipid content and composition of iPLA$_2$β-null and wild-type macrophages are actually similar or identical. The MS/MS data that permit assignment of the identities of GPC lipid molecular species are explained in Supplemental Results, and Table S1 contains quantitative data.

It could nonetheless be argued that iPLA$_2$β-null macrophages maintain a GPC lipid composition similar to that of wild-type cells by compensatory mechanisms that cause reciprocal changes in other classes of lipids that might affect sensitivity to free cholesterol loading-induced apoptosis. Accumulation of sphingomyelin (SM) and phosphatidylcholine (PC) are reciprocally regulated by SM synthase (86-89). If PC metabolism were perturbed, iPLA$_2$β-null cells might compensate by altering sphingolipid metabolism in order to preserve an optimal PC content and composition. SM avidly binds cholesterol (90), and the SM content of mouse peritoneal macrophages affects their ability to survive cholesterol loading (91). Figure S1 compares sphingolipids of peritoneal macrophages from wild-type and iPLA$_2$β-null mice and reveals no major differences between the two genotypes.

Polyunsaturated fatty acids initially incorporated into GPC lipids can be transferred subsequently to other phospholipid classes (60,92), and these processes might be altered iPLA$_2$β-null cells to preserve an optimal GPC lipid content and composition. Figures S2 and S3 compare the content and composition of glycerophospho-ethanolamine (GPE), -glycerol (GPG), -serine (GPS), and -inositol (GPI) lipid species in wild-type and iPLA$_2$β-null macrophages and reveal no major differences between the two genotypes.

Another possibility is that iPLA$_2$β-null macrophages differ from wild-type cells in their ability to internalize lipids in Ac-LDL and that this affects their ability to survive lipid-loading conditions that induce apoptosis in wild-type macrophages. Figure S4 and Table S2 compare effects of incubation with Ac-LDL and ACAT inhibitor 58035 on GPC lipids and sphingolipids in wild-type and iPLA$_2$β-null macrophages and reveal no major differences between the two genotypes.

Although the global phospholipid composition of wild-type and iPLA$_2$β-null macrophages are virtually identical, it could be argued that specific perturbation of the mitochondrial lipid composition could confer differential susceptibility to apoptosis in view of reports that interactions between iPLA$_2$β and mitochondrial are involved in apoptosis (78-81,96). Figure S5 illustrates that the mitochondrial sphingomyelin and GPC lipid compositions of wild-type and iPLA$_2$ß-null macrophages are essentially identical, however. Table S3 summarizes the identities of these lipid molecular species, and Table S4 illustrates that induction of ER stress by incubating macrophages with thapsigargin causes a decline in the mitochondrial content of GPC, GPE, and GPG lipid species in wild-type but not iPLA$_2$ß-null macrophages, suggesting that iPLA$_2$β might participate in the ER stress-induced mitochondrial phospholipid loss in wild-type cells.

Together, these observations indicate that differential susceptibility of peritoneal macrophages from wild-type and iPLA$_2$β-null mice to apoptosis induced by ER stress is not likely to be attributable to differences between the genotypes in cellular or mitochondrial lipid composition or lipid internalization.

SUPPLEMENTAL EXPERIMENTAL PROCEDURES

Positive ion electrospray ionization tandem mass spectrometric analyses of lysophosphatidylcholine species and the sphingolipids ceramide and sphingomyelin. Constant neutral loss (CNL) scanning was performed to monitor LPC $[M+Li]^+$ ions that undergo loss of 59 (trimethylamine) upon CAD. Quantitation was achieved by comparing the intensity of the 19:0-LPC internal standard ion (m/z 544) to intensities of ions for the endogenous species 14:0-LPC (m/z 474), 16:0-LPC (m/z 502), 18:0-LPC (m/z 530), 18:1-LPC (m/z 528), 18:2-LPC (m/z 526), and 20:4-LPC (m/z 550). Standard curve experiments in which a constant amount of 19:0-GPC and varied amounts of standard 14:0-. 16:0-, 18:1-, 18:0- and 20:4-LPC were added to a series of tubes and analyzed as Li^+ adducts by ESI/MS/MS indicated linearity over a wide concentration range that includes levels in mouse macrophages. Sphingomyelin and ceramide were visualized by ESI/MS/MS scanning for CNL of 59 and 48, respectively (46,105).

Electrospray ionization mass spectrometric analyses of anionic glycerophospholipids. Glycerophospho-ethanolamine (GPE), -glycerol (GPG), -serine (GPS), and -inositol (GPI), were analyzed as $[M-H]^-$ ions by ESI/MS(/MS) under described conditions relative to internal standards (45), and their tandem spectra were obtained using previously reported instrumental parameters (71).

SUPPLEMENTAL RESULTS

Rationalization of the tandem mass spectra of 16:0/16:0-GPC and of 16:0/18:1-GPC in Figures 10C and 10D and summary of the amounts of various GPC lipid molecular species in wild-type and iPLA$_2$β-null macrophages. The tandem spectrum in Figure 10C identifies the ion at *m/z* 740 in Figure 9 as the Li^+ adduct of 16:/0/16:0-GPC, as reflected by ions representing neutral losses of trimethylamine plus the fatty acid substituent ($M+Li^+$- 315) as a free fatty acid at *m/z* 425, and by losses of the fatty acid substituent from $[M+Li]^+$ as a free fatty acid (*m/z* 484) or as Li^+ salt (*m/z* 478), respectively.

The ion at *m/z* 766 in Figure 9 represents 16:0/18:1-GPC $[M+Li]^+$, as shown by its tandem spectrum (Figure 10D). Loss of trimethylamine (MLi^+-59) yields the ion *m/z* 707, and the ions *m/z* 583 (MLi^+-183) and *m/z* 577 (MLi^+-189) reflect net loss of $[HPO_4(CH_2)_2N(CH_3)_3]$ or $[LiPO_4(CH_2)_2N(CH_3)_3]$, respectively, and identify the head-group (67-69). Figure 10D also contains ions *m/z* 484, 478, and 425 that identify oleate as a fatty acid substituent. Those ions reflect neutral losses of oleic acid (M+Li - 282), of Li^+-oleate (M+Li - 288), and of trimethylamine plus oleic acid (M+Li - 341), respectively. Palmitate is the other fatty acid substituent of the parent $[M+Li]^+$ ion in Figure 10D, as shown by ions reflecting losses of palmitic acid (*m/z* 510), of Li^+-palmitate (*m/z* 504), and of trimethylamine plus palmitic acid (*m/z* 451). The relative abundance of ions *m/z* 425 and 451 in Figure 10D indicates that palmitate and oleate are the *sn*-1 and *sn*-2 substituents, respectively. The ion reflecting loss of trimethylamine plus the *sn*-1 substituent is more abundant than the ion reflecting loss of trimethylamine plus the *sn*-2 substituent in GPC lipid-Li^+ CAD spectra (67-69).

Table S1 contains quantitative data on the amounts of individual GPC lipid molecular species and reveals no major differences between wild-type and iPLA$_2$β-null macrophages.

Sphingolipid composition of peritoneal macrophages from wild-type and iPLA$_2$β-null mice. The ion at *m/z* 709 in Figure S1 represents the Li^+ adduct of the sphingomyelin (SM) species with palmitate as the fatty acid substituent (16:0-SM). Upon CAD, Li^+ adducts of SM species undergo facile elimination of trimethylamine (105). ESI/MS/MS scanning for constant neutral loss of 59 therefore accentuates the prominence of ions that represent SM species relative to those that represent PC species, as illustrated in Figures S1A and S1B. The two most abundant SM species in mouse peritoneal macrophages are 16:0-SM

(*m/z* 709) and 24:1-SM (*m/z* 819), and the relative abundances and absolute quantities of these compounds are similar in wild-type (Figure S1A) and iPLA$_2$β-null peritoneal macrophages (Figure S1B).

The sphingolipid ceramide (CM) can be produced by hydrolytic removal of the phosphocholine head-group from SM by sphingomyelinases, or CM can be converted to SM by SM synthase, which transfers the phosphocholine moiety from PC to CM (106). Upon CAD, Li^+ adducts of CM species readily undergo consecutive losses of water and formaldehyde for a net loss of 48 Th (107). ESI/MS/MS scanning for CNL of 48 therefore accentuates the prominence of ions that represent CM species, and, in conjunction with a non-naturally occurring internal standard, can be used to quantitate CM (46).

The ESI/MS/MS scans for CNL of 48 in Figures S1C and S1D illustrate that the two most prominent endogenous CM species in mouse peritoneal macrophages are represented by ions at *m/z* 544 and *m/z* 654 that correspond to Li^+ adducts of the species with palmitate (16:0-CM) or nervonate (24:1-CM), respectively, as fatty acid substituent. The ion at *m/z* 432 represents the non-naturally occurring internal standard 8:0-CM used to quantitate CM species, and the relative abundances and absolute quantities of CM species in iPLA$_2$β-null peritoneal macrophages (Figure S1D) is similar to that in wild-type macrophages (Figure S1C). Figure S1 thus illustrates that homozygous disruption of the mouse iPLA$_2$β gene does not result in obvious alteration of the content or composition of the sphingolipids CM and SM in peritoneal macrophages, and Table S2 summarizes quantitative data on macrophage sphingolipid content.

Electrospray ionization mass spectrometric analyses of glycerophospho-ethanolamine (GPE), -glycerol (GPG), -serine, and -inositol (GPI) lipid species in wild-type and iPLA$_2$β-null peritoneal macrophages. Negative ion ESI/MS analyses of lipid extracts from wild-type (Figure S2A) and iPLA$_2$β-null (Figure S2B) peritoneal macrophages infused in solutions with little salt and no added base revealed abundant ions that represent 16:0/18:1-GPG (*m/z* 747), 18:1/18:1-GPG (*m/z* 773), 18:0/18:1-GPS (*m/z* 788), 18:0/20:4-GPS (*m/z* 810), 18:0, 22:6-GPS (*m/z* 834), 18:0/18:1-GPI (*m/z* 863), 18:0/20:4-GPI (*m/z* 885), and 18:0/22:5-GPI (*m/z* 911). The identities of the species represented by various ions were determined from their tandem spectra, as described below, and the ESI/MS profiles of these lipids from wild-type macrophages (Figure S2A) are similar to that for iPLA$_2$β-null macrophages (Figure S2B).

The composition of the solution in which glycerolipid analytes are infused into the ESI/MS/MS source can be manipulated to favor or suppress ionization of selected head-group classes (77). Adding LiOH to the solution suppresses ionization of GPG, GPS, and GPI lipids and enhances that of GPE lipids, as illustrated in Figures S2C and S2D. The major GPE lipid $[M-H]^-$ ions from mouse macrophages included plasmalogen (plasmenylethanolamine) species 16:0p/18:1-GPE (*m/z* 700), 16:0p/20:4-GPE (*m/z* 722), 18:2p/20:4-GPE (*m/z* 746), 18:1p/20:4-GPE (*m/z* 748), 18:0p/20:4-GPE (*m/z* 750), and 18:0p/22:6 (*m/z* 774). All of these ions disappeared when the lipid solutions were acid-treated before infusion (not shown), consistent with the acid-lability of the plasmalogen *sn*-1 vinyl ether linkage (108).

The major diacyl GPE (phosphatidylethanolamine) species in wild-type macrophage lipid extracts (Figure S2C) included 18:0/18:2-GPE (*m/z* 742), 18:0/20:4-GPE (*m/z* 766), 18:0/22:6-GPE (*m/z* 790), 18:0/22:5-GPE (*m/z* 792), and 18:0/22:4-GPE (*m/z* 794). The ion at *m/z* 662 represents the internal standard 15:0/15:0-GPE used to quantitate GPE species, and the relative abundances and absolute quantities of the GPE species in iPLA$_2$β-null peritoneal macrophages (Figure S2D) are nearly identical to those in wild-type macrophages (Figure S2C). There is no deficiency of arachidonate-containing GPE lipid species in the iPLA$_2$β-null macrophages, and this is further illustrated by the quantitative data in Table S1 on individual GPE lipid molecular species.

Identities of lipid species represented by ions in Figure S2 were determined from their tandem mass spectra (Figure S3). In the tandem spectrum of 16:0/18:1-GPG (Figure S3A), the head-group is identified by the ions *m/z* 171 (glycerol-phosphate) and *m/z* 153 (loss of H_2O from *m/z* 171) (109). The fatty acid substituents are identified by palmitate (*m/z* 255) and oleate (*m/z* 281) anions. The positions of the fatty acids on the glycerol backbone are established by the fact that ions representing neutral loss of the *sn*-2 substituent as a free fatty acid (*m/z* 465) or as a ketene (*m/z* 483) are more abundant than ions

representing corresponding losses of the *sn*-1 substituent (*m/z* 491 and *m/z* 509, respectively) (109). An ion characteristic of the glycerol head-group (*m/z* 391) represents loss of glycerol from *m/z* 483 (109).

In the tandem mass spectrum of 18:0/20:4-GPS (Figure S3B), the head group is identified by *m/z* 723, which represents loss of a dehydration product of serine from $[M-H]^-$. Fatty acid substituents are identified by their carboxylate anions at *m/z* 283 (18:0) and 303 (20:4). Positions of fatty acids on the glycerol backbone are established by the fact that ions reflecting loss of the *sn*-2 substituent (arachidonate) as a free fatty acid (*m/z* 419) or as a ketene (*m/z* 437) are more abundant than ions reflecting corresponding losses of the *sn*-1 substituent (110).

In the tandem mass spectrum of 18:0/20:4-GPI (Figure S3C), the head group is identified by the ions of *m/z* 241, which represents a dehydration product of inositol phosphate, and of *m/z* 223 (loss of H_2O from *m/z* 241) (111). Fatty acid substituents are identified by their carboxylate anions at *m/z* 283 (18:0) and 303 (20:4). Positions of the fatty acids on the glycerol backbone are established by the fact that ions reflecting loss of the *sn*-2 substituent (arachidonate) as a free fatty acid (*m/z* 581) or as a ketene (*m/z* 599) are more abundant than ions reflecting corresponding losses of the *sn*-1 substituent (*m/z* 601 and 619, respectively) (111). An ion characteristic of the inositol head-group (*m*/z 419) represents loss of inositol from *m/z* 599 (111).

In the tandem mass spectrum of 16:0p/20:4-GPE (Figure S3D), the single fatty acid substituent is identified by arachidonate (*m/z* 303) anion and by ions representing losses of that substituent as a free fatty acid (*m/z* 418) or as a ketene (*m/z* 436). This material is acid-labile, as is typical of plasmalogens (108), and its tandem spectrum is consistent with 16:0p/20:4-GPE (112) and identical to that previously reported for that compound (108). The spectra in Figures S2 and S3 thus illustrate that macrophages from iPLA$_2$β-null mice exhibit no obvious abnormalities in the content or composition of anionic glycerophospholipids in the head-group classes GPE, GPG, GPS, or GPI.

Ac-LDL loading-induced changes in macrophage content of lysophosphatidylcholine, phosphatidylcholine, sphingomyelin, and ceramide. To determine effects of Ac-LDL loading on macrophage LPC content, ESI/MS/MS scanning was performed (Figure S4). After incubating macrophages with or without Ac-LDL and ACAT inhibitor 58035, internal standard 19:0-LPC, which does not occur naturally in mouse peritoneal macrophages, was added to macrophage lipid extracts, and LPC species were isolated by TLC and analyzed as Li^+ adducts by ESI/MS/MS scanning for CNL of trimethylamine (loss of 59) (69). This approach yields a better signal to noise ratio than does monitoring total ion current (60,70). Comparing relative intensities of ions for 19:0-LPC-Li^+ (*m/z* 544) and endogenous species, such as 16:0-LPC-Li^+ (*m/z* 502) and 18:0-LPC-Li^+ (*m/z* 530) yields a linear standard curve over a wide concentration range that includes LPC levels observed in macrophages. Figure S4A illustrates that abundant LPC species in wild-type mouse peritoneal macrophages include 16:0-LPC (*m/z* 502) and three 18-carbon LPC species with varying degrees of unsaturation of the fatty acid side chain (*m/z* 530, 528, and 526). Loading wild-type macrophages with Ac-LDL induces an increase in endogenous LPC species relative to the internal standard (Figure S4B).

A series of similar experiments indicated that total resting LPC mass in wild-type macrophages is not significantly different from that in iPLA$_2$β-null macrophages (Table S2). Loading wild-type or iPLA$_2$β-null macrophages with Ac-LDL in the presence of ACAT inhibitor 58035 induced a several-fold rise in total LPC content that was about twice as great as that induced by Ac-LDL alone (Table S2). Ac-LDL loading also induced similar increases in the PC content of wild-type and iPLA$_2$β-null macrophages, and again the increases were greater in the presence than in the absence of the ACAT inhibitor (Table S2). Interestingly, Ac-LDL loading induced many-fold rises in content of the sphingolipids ceramide and sphingomyelin in wild-type and iPLA$_2$β-null macrophages in the absence of the ACAT inhibitor but much smaller rises in the presence of the inhibitor (Table S2). The only significant differences between the two genotypes in their lipid content were that iPLA$_2$β-null macrophages exhibited a slightly higher basal CM content and achieved a somewhat higher PC content after incubation with both Ac-LDL and ACAT inhibitor 58035 than did wild-type macrophages. Macrophages of both genotypes experienced

significant increases in their PC, LPC, and CM content upon lipid-loading, suggesting that lipid internalization mechanisms are not defective in iPLA$_2$β-null macrophages.

Mitochondrial phospholipid composition of wild-type and iPLA$_2$β-null mouse macrophages. Annotation in Figure S5 specifies the identities of the most prominent macrophage mitochondrial sphingomyelin and GPC lipid species by their fatty acid substituents and backbone/headgroup structure, and Table S3 provides a summary of these and less abundant species. Figures S5C and S5D represent ESI/MS/MS scans for constant neutral loss of 189, which selectively display GPC lipids (67-69), for mitochondrial extracts from wild-type and iPLA$_2$β-null macrophages, respectively and display some species that are obscured in total ion current tracings. The mitochondrial lipid profiles for wild-type (Panels A and C) and iPLA$_2$β-null macrophages are essentially identical in both sets of analyses. Table S4 illustrates that incubating wild-type macrophages with thapsigargin induced a decline in mitochondrial GPC, GPE, and GPG lipid content upon positive and negative ESI/MS analyses relative to internal standards, but little change in these lipids occurred with iPLA$_2$β-null macrophage mitochondria. Mitochondrial sphingomyelin content was little affected in either wild-type or iPLA$_2$β-null macrophages upon incubation with thapsigargin.

SUPPLEMENTAL REFERENCES

105. Hsu, F.F., and Turk, J. (2000) *J. Am. Soc. Mass Spectrom.* **11**, 437-449
106. Kolesnick, R. (2002) *J. Clin. Invest.* **110**, 3-8
107. Hsu, F.F., Turk, J., J, Stewart, M.E., Downing, D.T. (2002) *J. Am. Soc. Mass Spectrom.* **13**, 680-695
108. Ramanadham, S., Hsu, F.F., Bohrer, A., Nowatzke, W., Ma, Z., and Turk, J. (1998) *Biochemistry* **37**, 4533-4567
109. Hsu, F.F., and Turk, J. (2001) *J. Am. Soc. Mass Spectrom.* **12**, 1036-1043
110. Hsu, F.F., and Turk, J. (2005) *J. Am. Soc. Mass Spectrom.* **16**, 1510-1522
111. Hsu, F.F., and Turk, J. (2000) *J. Am. Soc. Mass Spectrom.* **11**, 986-999
112. Hsu, F.F., and Turk, J. (2000 *J. Am. Soc. Mass Spectrom.* **11**, 892-899

SUPPLEMENTAL FIGURE LEGENDS

Supplemental Figure 1. ESI/MS/MS analyses of the sphingolipids sphingomyelin and ceramide from mouse peritoneal macrophages. Lipid extracts from wild-type (Panels A and C) or iPLA$_2$β-null (Panels B and D) macrophages were analyzed by ESI/MS/MS scanning for constant neutral loss of 59 (Panels A and B) or of 48 (Panels C and D) to accentuate prominence of ions from Li^+ adducts of sphingomyelin (Panels A and B) or of ceramide (Panels C and D) molecular species relative to other components.

Supplemental Figure 2. Negative ion electrospray ionization mass spectrometric analyses of anionic glycerophospholipid species in peritoneal macrophages from wild-type and iPLA$_2$β-null mice. Lipids were extracted from wild-type (Panels A and C) or iPLA$_2$β-null (Panels C and D) macrophages without (Panels A and B) or with (Panels C and D) added LiOH and analyzed by negative ion ESI/MS. Under the former condition, ionization of GPG, GPS, and GPI lipids is enhanced and that of GPE lipids is suppressed. Under the latter condition, ionization of GPE lipids is enhanced and that of GPG, GPS, and GPI lipids is suppressed. Total negative ion current is plotted *vs. m/z* value.

Supplemental Figure 3. Tandem mass spectra of anionic glycerophospholipids from mouse peritoneal macrophages. Phospholipids were extracted from wild-type or iPLA$_2$β-null macrophages and analyzed by negative ion ESI/MS/MS. Specific ions were selected in the first quadrupole and accelerated into the

collision cell to induce CAD. Product ions were analyzed in the final quadrupole. Ions selected in the first quadrupole included *m/z* 747 (Panel A), 810 (Panel B), 885 (Panel C), and 722 (Panel D).

Supplemental Figure 4. Electrospray ionization tandem mass spectrometric analyses of the lysophosphatidylcholine (LPC) content wild-type macrophages incubated without or with acetylated LDL and an ACAT inhibitor. After incubating (24 hr) wild-type macrophages without (Panel A) or with Ac-LDL and ACAT inhibitor 58035, phospholipids were extracted, mixed with internal standard 19:0-LDL, and analyzed by positive ion ESI/MS/MS scanning for constant neutral loss of 59 from Li^+ adducts.

Supplemental Figure 5. Mitochondrial glycerophosphocholine lipids and sphingomyelin species of wild-type and iPLA$_2$β-null mouse macrophages. Mitochondria were isolated from wild-type (Panels A and C) or iPLA$_2$β-null (Panels B and D) macrophages, and their lipids were extracted, mixed with internal standard 14:0/14:0-GPC, and analyzed as Li^+ adducts by ESI/MS (Panels A and B) or by ESI/MS/MS scanning for constant neutral loss of 189 (Panels C and D). Identities of the sphingomyelin and GPC lipid species represented by various ions in the spectra are summarized in Table S3.

SUPPLEMENTAL TABLES

Supplemental Table 1. Quantities of molecular species of GPC lipids and GPE lipids in peritoneal macrophages from wild-type and iPLA$_2$β-null mice. Phospholipids were extracted from wild-type or iPLA$_2$β-null macrophages and analyzed by ESI/MS as in Fig. 9 (positive ions for GPC lipids as $[M+Li]^+$ ions) and Figure S3 (negative ions for GPE lipid $[M-H]^-$ ions) relative to the internal standards 14:0/14:0-GPC or 15:0/15:0-GPE, respectively, and quantities were determined from abundances of ions of appropriate *m/z* value for the indicated molecular species relative to that for the internal standard by interpolation from a standard curve. Mean values ± SEM are displayed (n = 3). The designation "p" denotes a plasmalogen, which contains a vinyl ether linkage in the *sn*-1 position.

GPC species	Wild-Type pmol/nmol	iPLA$_2$β$^{-/-}$ pmol/nmol	Wild-Type per cent	iPLA$_2$β$^{-/-}$ per cent	GPE species	Wild-Type pmol/nmol	iPLA$_2$β$^{-/-}$ pmol/nmol	Wild-Type per cent	iPLA$_2$β$^{-/-}$ per cent
16:0/16:0	151 ± 3.5	166 ± 4.2	20.5 ± 0.5	21.2 ± 0.5	**16:0p/20:4**	23.6 ± 1.4	34.5 ± 2.9	16.5 ± 1.0	17.6 ± 1.5
16:0/18:2	135 ± 2.8	148 ± 2.9	18.4 ± 0.4	18.0 ± 0.4	**18:0/18:2**	14.7 ± 0.9	22.7 ± 1.8	10.3 ± 0.6	11.4 ± 0.9
16:0/18:1	81.3 ± 1.7	86.0 ± 2.3	11.0 ± 0.2	11.0 ± 0.3	**18:0/18:1**	9.04 ± 0.4	10.4 ± 0.7	6.33 ± 0.3	5.22 ± 0.4
16:0/20:4	71.8 ± 1.5	75.5 ± 1.7	9.73 ± 0.2	9.65 ± 0.2	**16:0p/22:6**	14.2 ± 0.7	19.2 ± 1.4	9.96 ± 0.5	9.64 ± 0.7
18:1/18:2	79.6 ± 1.6	78.0 ± 1.7	10.8 ± 0.2	9.97 ± 0.2	**18:1p/22:6**	20.5 ± 1.2	28.3 ± 2.2	14.3 ± 0.8	14.2 ± 1.1
18:0/18:2	98.0 ± 2.0	103 ± 2.4	13.3 ± 0.3	13.2 ± 0.3	**18:0p/20:4**	19.3 ± 1.1	27.8 ± 2.3	13.5 ± 0.8	14.0 ± 1.2
16:0/22:6	34.5 ± 0.6	35.0 ± 0.9	4.68 ± 0.1	4.47 ± 0.1	**16:0/22:6**	3.91 ± 0.2	5.25 ± 0.3	2.74 ± 0.1	2.64 ± 0.1
18:1/20:4	36.7 ± 0.8	38.4 ± 0.9	4.97 ± 0.1	4.91 ± 0.1	**18:1/20:4**	4.83 ± 0.2	5.83 ± 0.3	3.38 ± 0.2	2.93 ± 0.2
18:0/20:4	49.0 ± 0.9	52.5 ± 1.0	6.64 ± 0.1	6.71 ± 0.1	**18:0/20:4**	13.6 ± 0.7	19.4 ± 1.3	9.50 ± 1.9	9.75 ± 0.7
					18:1p/22:6	5.35 ± 0.3	6.79 ± 0.4	3.75 ± 0.2	3.4 ± 0.2
					18:0p/22:6	7.89 ± 0.5	10.2 ± 0.7	5.52 ± 0.3	5.15 ± 0.4
					18:0/22:6	5.96 ± 0.3	8.02 ± 0.4	4.17 ± 0.2	4.03 ± 0.2

Supplemental Table 2. Changes in the content of GPC lipids and sphingolipids in wild-type and iPLA$_2$β-null mouse peritoneal macrophages induced by incubation with Ac-LDL in the presence or absence of ACAT inhibitor 58035. Wild-type or iPLA$_2$β-null macrophages were incubated with Ac-LDL in the presence or absence of ACAT inhibitor 58035 as in Fig. 2, and phospholipids were extracted and analyzed by ESI/MS relative to internal standards as in Fig. 9-12, S2, and S5. PC denotes phosphatidylcholine; LPC, lysophosphatidylcholine; SM, sphingomyelin; and CM, ceramide. Quantities of individual molecular species were determined as in Table S1, and the sum of species within each lipid class was computed. Mean values ± S.E.M. are expressed as nmol/10^6 cells (n = 3).

GENOTYPE	**Wild-Type**	**Wild-Type**	**Wild-Type**	**iPLA$_2$β-null**	**iPLA$_2$β-null**	**iPLA$_2$β-null**
ANALYTE	**PC**	**PC**	**PC**	**PC**	**PC**	**PC**
CONDITION	**CONTROL**	**AcLDL**	**AcLDL+58035**	**CONTROL**	**AcLDL**	**AcLDL+58035**
MEAN ± SEM	3.43 ± 0.55	11.01 ± 2.99	21.01 ± 2.47	4.41 ± 0.83	14.79 ± 3.64	31.33 ± 0.77
RATIO/CON	1.00 ± 0.16	3.22 ± 0.87	6.14 ± 0.72	1.00 ± 0.19	3.36 ± 0.82	7.11 ± 0.17
p vs. WT	na	na	na	0.380	0.467	0.016
p vs. CON	na	0.067	0.002	na	0.050	<0.001
GENOTYPE	**Wild-Type**	**Wild-Type**	**Wild-Type**	**iPLA$_2$β-null**	**iPLA$_2$β-null**	**iPLA$_2$β-null**
ANALYTE	**LPC**	**LPC**	**LPC**	**LPC**	**LPC**	**LPC**
CONDITION	**CONTROL**	**AcLDL**	**AcLDL+58035**	**CONTROL**	**AcLDL**	**AcLDL+58035**
MEAN ± SEM	0.13 ± 0.09	0.64 ± 0.22	1.36 ± 0.30	0.26 ± 0.10	1.22 ± 0.10	2.35 ± 0.26
RATIO/CON	1.00 ± 0.09	5.04 ± 1.71	10.69 ± 2.36	1.00 ± 0.73	6.00 ± 0.47	11.57 ± 1.28
p vs. WT	na	na	na	0.689	0.072	0.067
p vs. CON	na	0.095	0.017	na	0.004	0.002
GENOTYPE	**Wild-Type**	**Wild-Type**	**Wild-Type**	**iPLA$_2$β-null**	**iPLA$_2$β-null**	**iPLA$_2$β-null**
ANALYTE	**SM**	**SM**	**SM**	**SM**	**SM**	**SM**
CONDITION	**CONTROL**	**AcLDL**	**AcLDL+58035**	**CONTROL**	**AcLDL**	**AcLDL+58035**
MEAN ± SEM	2.34 ± 0.51	9.71 ± 3.14	3.13 ± 1.81	1.90 ± 0.68	11.59 ± 3.92	5.01 ± 2.29
RATIO/CON	1.00 ± 0.22	4.15 ± 1.34	1.34 ± 0.77	1.00 ± 0.36	6.09 ± 2.06	2.63 ± 1.20
p vs. WT	na	na	na	0.636	0.727	0.555
p vs. CON	na	0.082	0.696	na	0.071	0.264
GENOTYPE	**Wild-Type**	**Wild-Type**	**Wild-Type**	**iPLA$_2$β-null**	**iPLA$_2$β-null**	**iPLA$_2$β-null**
ANALYTE	**CM**	**CM**	**CM**	**CM**	**CM**	**CM**
CONDITION	**CONTROL**	**AcLDL**	**AcLDL+58035**	**CONTROL**	**AcLDL**	**AcLDL+58035**
MEAN ± SEM	0.07 ± 0.01	2.61 ± 1.73	1.38 ± 0.19	0.17 ± 0.02	3.37 ± 0.69	1.74 ± 0.211
RATIO/CON	1.00 ± 0.05	35.6 ± 5.19	18.82 ± 2.56	1.00 ± 0.13	19.42 ± 4.00	10.02 ± 1.22
p vs. WT	na	na	na	0.013	0.394	0.276
p vs. CON	na	0.003	0.002	na	0.010	0.002

Supplemental Table 3. Mouse peritoneal macrophage mitochondrial glycerophosphocholine lipids and sphingomyelin species. Macrophage mitochondria were isolated, and their lipids were extracted, and analyzed as Li^+ adducts by ESI/MS and then by ESI/MS/MS as in Fig. S5. SM denotes sphingomyelin and GPC glycerophosphocholine. The designation "e" denotes an *sn*-1 O-alkyl ether linkage.

Ion (*m/z*)	Predominant Species	Relative Abundance (%)
709	16:0-SM	90
726	16:0e/16:0-GPC	21
738	16:0/16:1-GPC	39
740	16:0/16:0-GPC	56
752	16:0e/18:1-GPC	28
764	16:0/18:2-GPC	49
766	16:0/18:1-GPC	100
788	16:0/20:4-GPC	15
790	18:1/18:2-GPC	42
792	18:0/18:2-GPC	70
794	18:0/18:1-GPC	30
816	18:0/20:4-GPC	23
819	24:1-SM	39

Supplemental Table 4. Changes in mitochondrial phospholipids from wild-type and iPLA$_2$β-null mouse peritoneal macrophages induced by incubation with thapsigargin. Wild-type or iPLA$_2$β-null macrophages were incubated (24 hr) with thapsigargin (0.5 μM), and mitochondria were isolated and their protein content determined. Phospholipids were extracted, mixed with internal standards, and analyzed by ESI/MS relative to internal standards as in Figure S5 (positive ions for PC and SM) and Figure S2 (negative ions for PE and PG). PC denotes phosphatidylcholine; SM, sphingomyelin; PE, phosphatidylethanolamine; and PG, phosphatidylglycerol. Values (mean ± S.E.M., n = 4) represent the sum of ion currents for members of each class normalized to internal standards for mitochondrial lipid extracts from thapsigargin-treated macrophages divided by that for untreated macrophages of each genotype. Ratios for wild-type cells were significantly ($p < 0.05$) lower than 1 for PC, PE, and PG. No ratios were significantly different from 1 for iPLA$_2$β-null cells.

Phospholipid Class	Wild-Type	iPLA$_2$β-Null
PC	0.77 ± 0.06	0.97 ± 0.07
SM	1.11 ± 0.02	0.93 ± 0.07
PE	0.57 ± 0.07	0.91 ± 0.10
PG	0.63 ± 0.08	0.97 ± 0.07

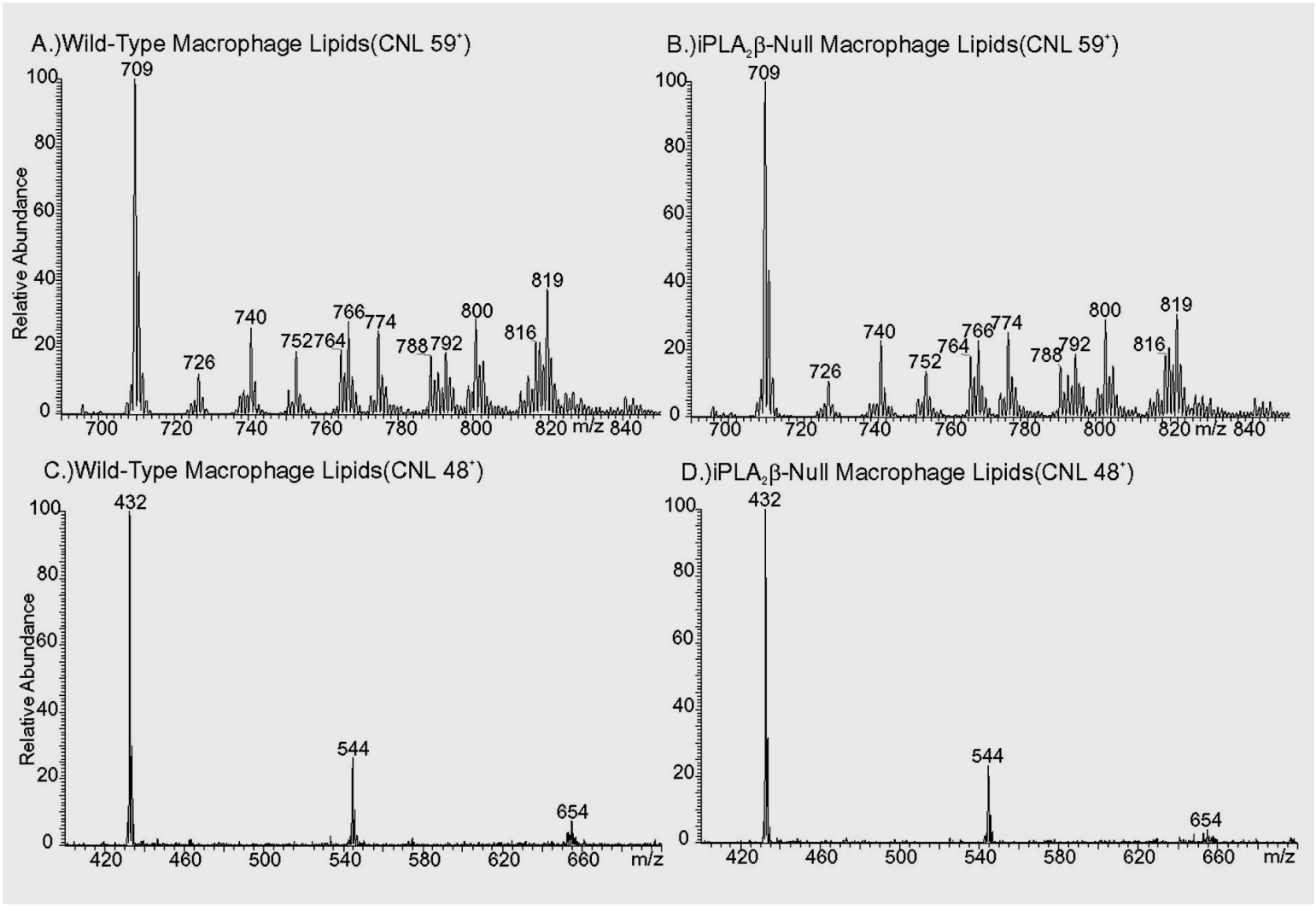
A.)Wild-Type Macrophage Lipids(CNL 59+)
B.)iPLA2β-Null Macrophage Lipids(CNL 59+)
C.)Wild-Type Macrophage Lipids(CNL 48+)
D.)iPLA2β-Null Macrophage Lipids(CNL 48+)
Relative Abundance
m/z
709
726
740
752
764
766
774
788
792
800
816
819
432
544
654

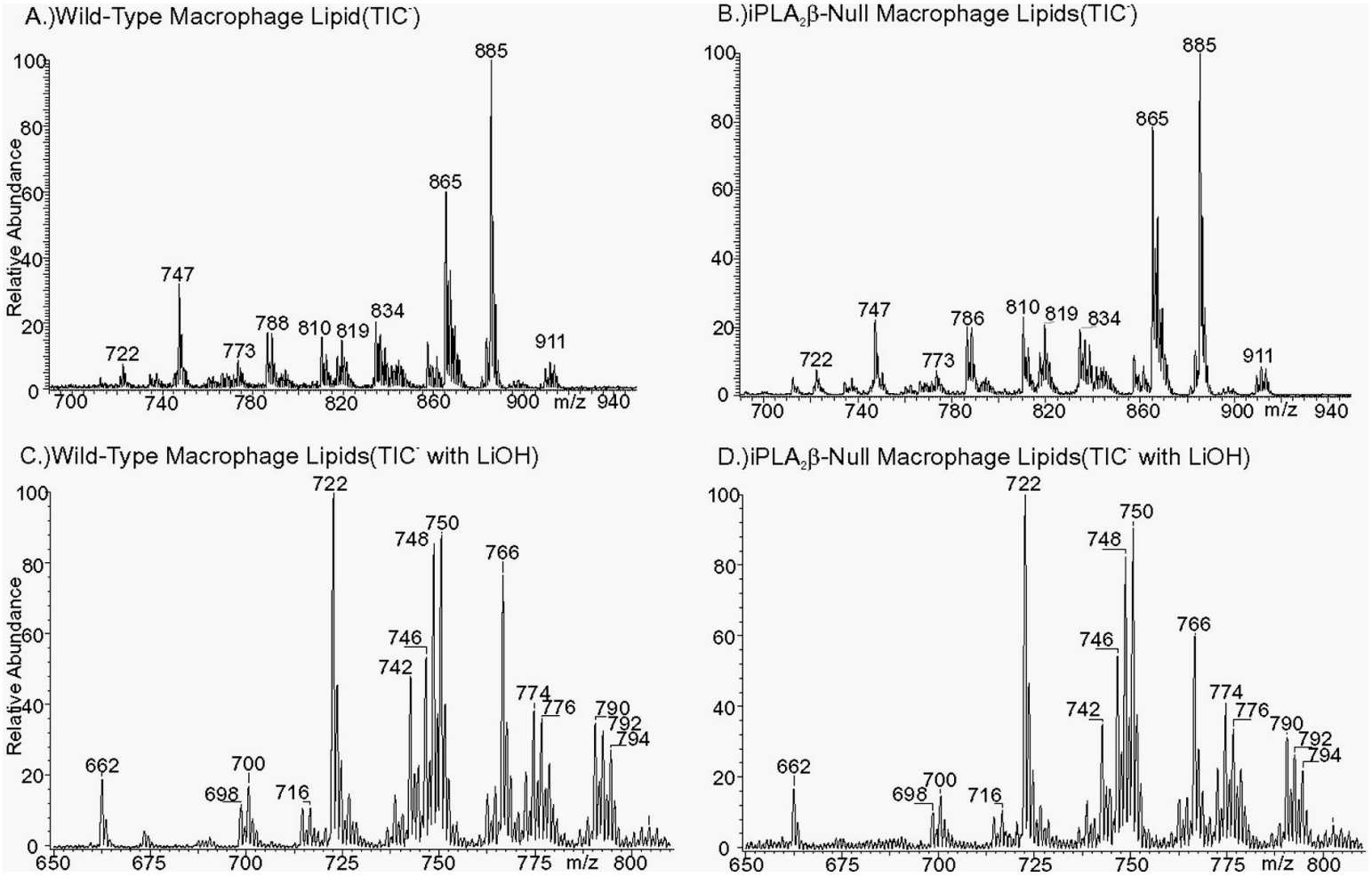
A.)Wild-Type Macrophage Lipid(TIC-)
B.)iPLA2β-Null Macrophage Lipids(TIC-)
C.)Wild-Type Macrophage Lipids(TIC- with LiOH)
D.)iPLA2β-Null Macrophage Lipids(TIC- with LiOH)
Relative Abundance
m/z
722
747
773
788
810
819
834
865
885
911
786
662
698
700
716
742
746
748
750
766
774
776
790
792
794

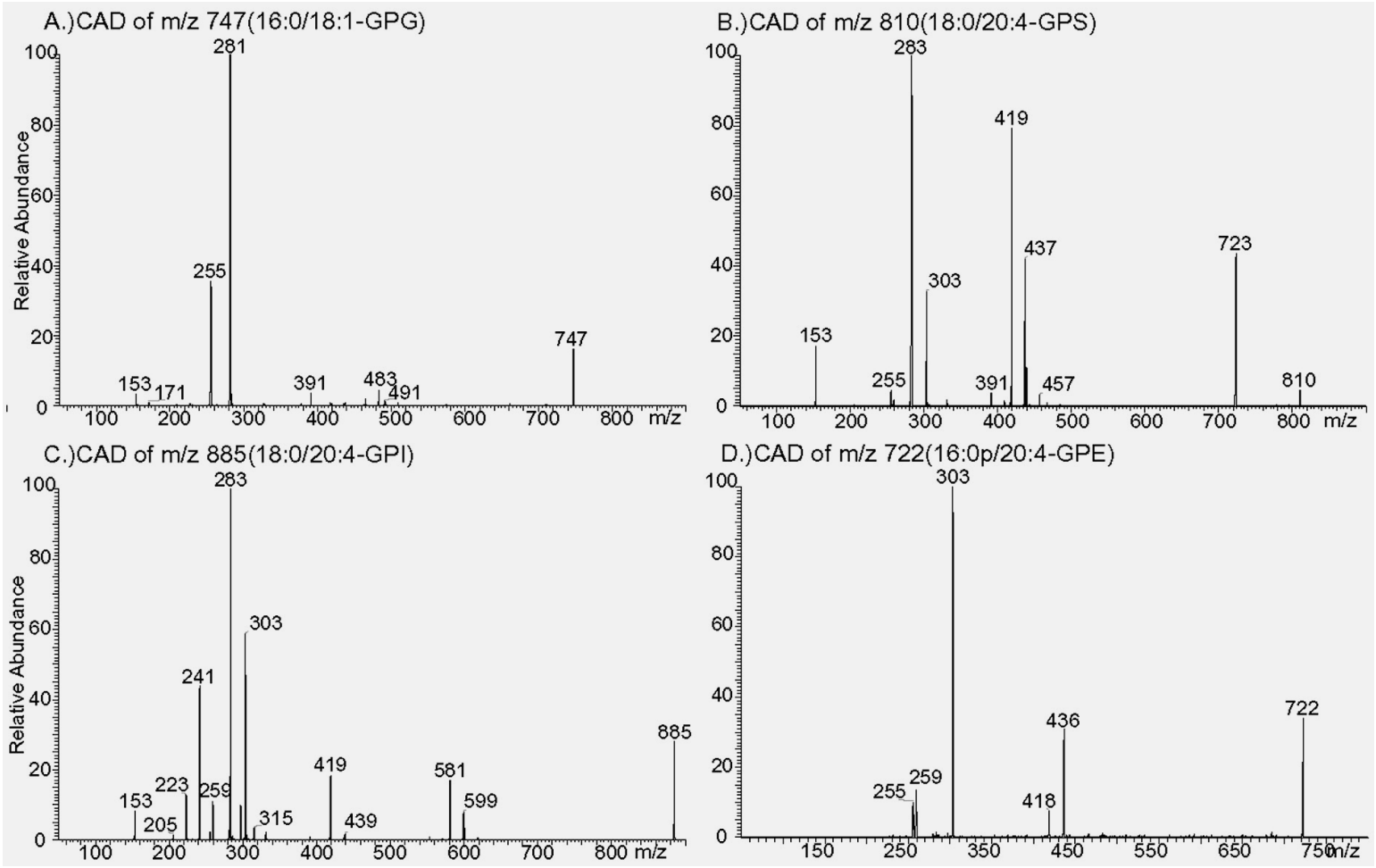
A.)CAD of m/z 747(16:0/18:1-GPG)
Relative Abundance
281
255
747
153
171
391
483
491
m/z
B.)CAD of m/z 810(18:0/20:4-GPS)
283
419
437
723
303
153
255
391
457
810
m/z
C.)CAD of m/z 885(18:0/20:4-GPI)
Relative Abundance
283
303
241
885
419
581
223
259
599
153
315
205
439
m/z
D.)CAD of m/z 722(16:0p/20:4-GPE)
303
722
436
259
255
418
m/z

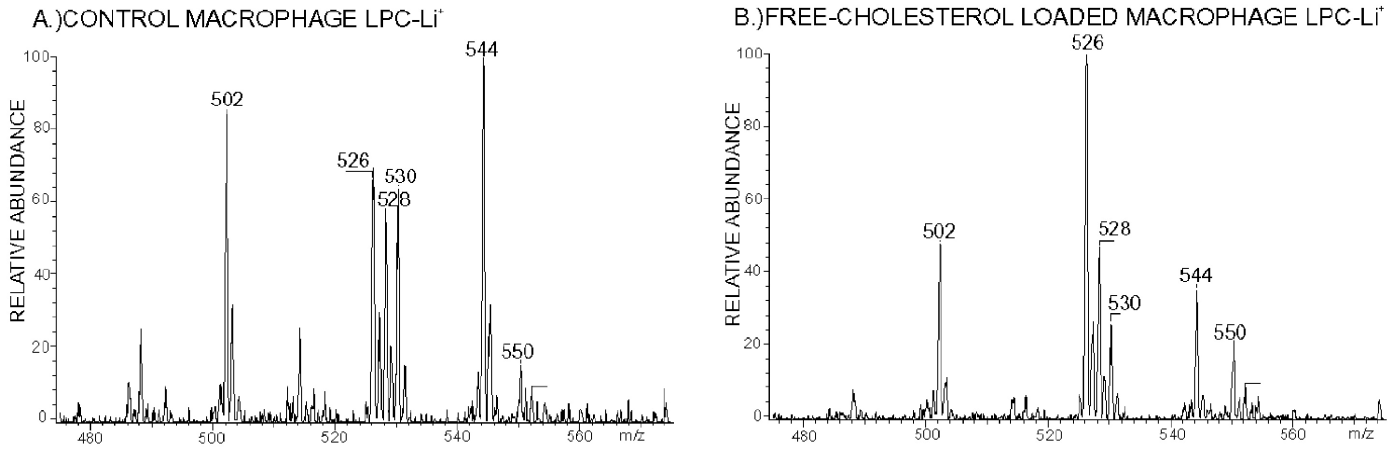
A.)CONTROL MACROPHAGE LPC-Li+
RELATIVE ABUNDANCE
100
80
60
40
20
0
480
500
520
540
560
m/z
502
526
528
530
544
550
B.)FREE-CHOLESTEROL LOADED MACROPHAGE LPC-Li+
RELATIVE ABUNDANCE
100
80
60
40
20
0
480
500
520
540
560
m/z
502
526
528
530
544
550

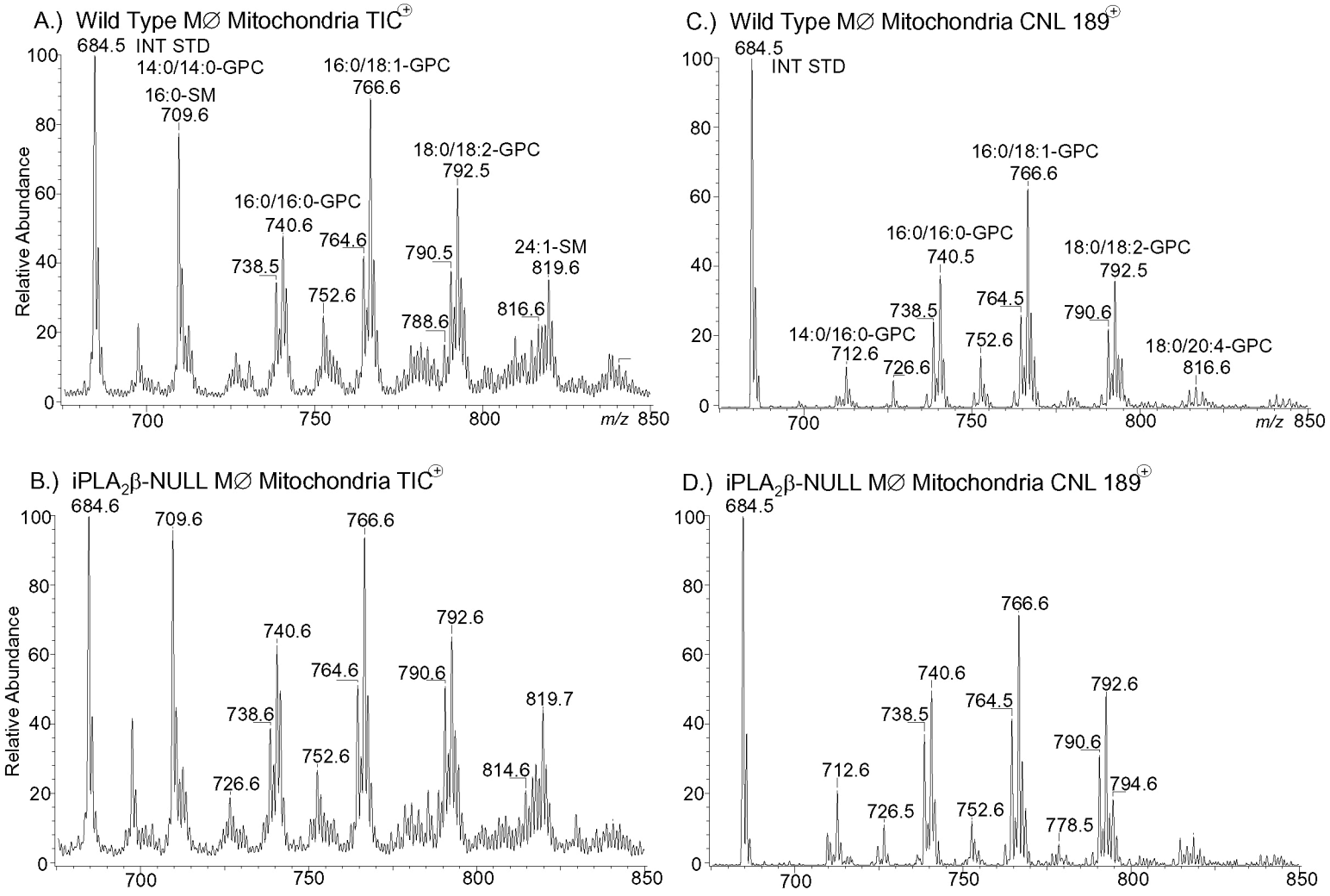
A.) Wild Type MØ Mitochondria TIC
684.5 INT STD
14:0/14:0-GPC
16:0-SM
709.6
16:0/18:1-GPC
766.6
18:0/18:2-GPC
792.5
16:0/16:0-GPC
740.6
764.6
738.5
752.6
790.5
24:1-SM
819.6
788.6
816.6
Relative Abundance
m/z
C.) Wild Type MØ Mitochondria CNL 189
684.5
INT STD
16:0/18:1-GPC
766.6
16:0/16:0-GPC
740.5
18:0/18:2-GPC
792.5
738.5
764.5
790.6
14:0/16:0-GPC
712.6
752.6
726.6
18:0/20:4-GPC
816.6
B.) iPLA2β-NULL MØ Mitochondria TIC
684.6
709.6
766.6
740.6
792.6
764.6
790.6
738.6
819.7
752.6
726.6
814.6
D.) iPLA2β-NULL MØ Mitochondria CNL 189
684.5
766.6
740.6
792.6
764.5
738.5
790.6
712.6
794.6
726.5
752.6
778.5